Lecture 4

A. Ionic Model for Bonding and the Role of Ionic Radii in Understanding the Partitioning of Trace Elements Between Phases

The usefulness of ionic radii in Trace Element Geochemistry was recognized by Goldschmidt who formulated the Goldschmidt Rules to describe partitioning of trace elements between solids and melt:

(1) If two ions have similar ionic radii and the same charge, the smaller ion will be preferentially concentrated in the solid;

(2) If two ions have similar radii but different charges, the ion with the higher charge will be preferentially concentrated in the solid.

These rules originate from a simple ionic model whereby solids (minerals) are viewed as an array of cations and anions with attractive and repulsive forces.

The concept of lattice energy, U, is a measure of the forces within an ionic crystal; it is a sum of attractive and repulsive forces.

$$\text{U} = \overbrace{\frac{-N\,|z^+z^-|\,Ae^2}{r}}^{\textit{attractive force}} + \overbrace{\frac{NBe^2}{r^n}}^{\textit{repulsive force}}$$

Where N = Avogrados number

Z = charge on ion

A = Madelung constant which reflects the geometric arrangement of anions and cations

e = charge on electron

r = interionic distance between cation and anion

B and n are constants, n = 8 to 10.

Since $\dfrac{dU}{dr} = 0$ when $r = r_o$, with r_o being the most favorable interionic distance.

$$U = \frac{-N\,|z^+z^-|\,Ae^2}{r_o}\left(1 - \frac{1}{n}\right) \qquad \text{[see Figure 4]}$$
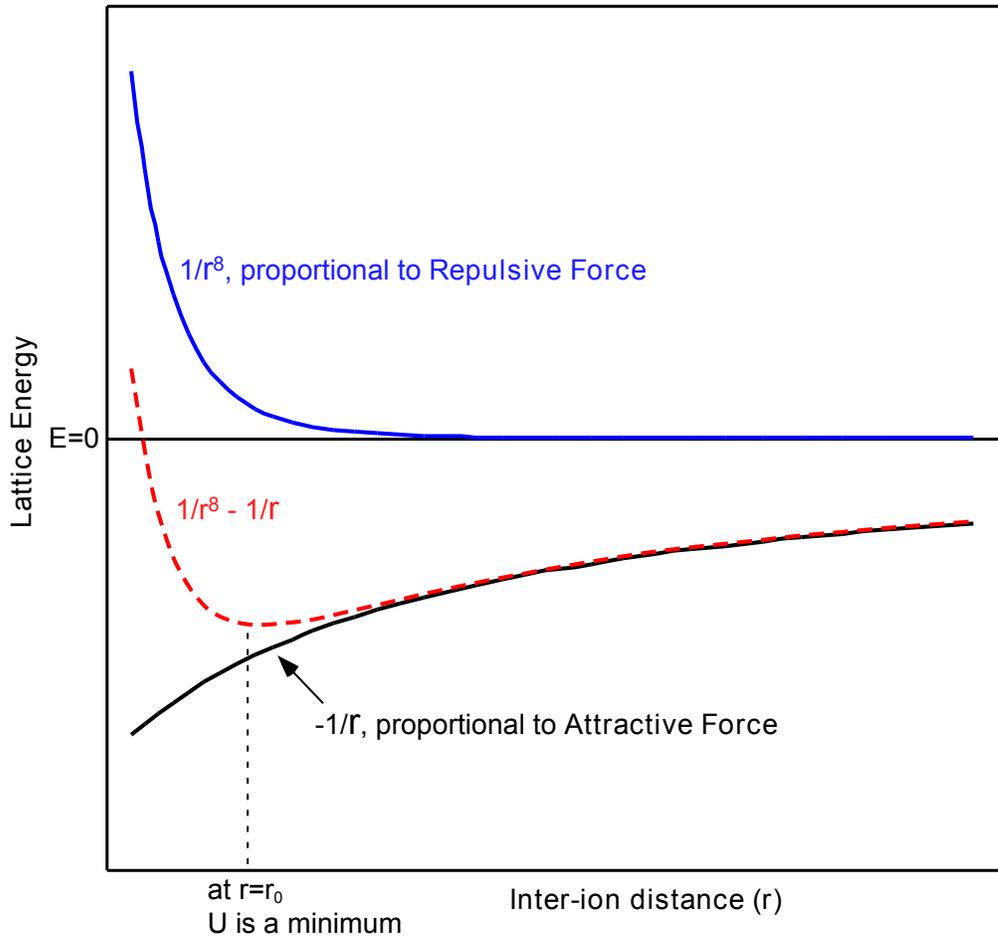
Figure 4: A plot of the two terms in the Lattice Energy equation, i.e. the attractive force varying as $1/r$ and the electron repulsion force varying as $1/r^8$, showing that there is an interionic distance (r_o) where the lattice energy is a minimum.

We see that Goldschmidt's Rules are based on the (z^+z^-) and $\dfrac{1}{r_o}$ terms; therefore the Goldschmidt's Rules arise from the concept of Lattice Energy which is at a minimum at an interionic distance equal to r_o (Figure 4). Also lattice energy is at a minimum in a system of spherical ions when each ion is surrounded by as many ions of opposite charge as possible; the number of nearest neighbors is defined as coordination number (CN).

2

We now know that Goldschmidt's Rules are not rigorously correct:

(1) We will learn that for a given structural site in a mineral, there is an optimal ionic radius and ions that are <u>too large</u> or <u>too small</u> are less readily incorporated into the mineral than an ion of optimal size.

(2) Highly charged ions are not always preferentially incorporated into solids, e.g., there are charge balance considerations.

(3) Partitioning involves two phases, and in solid-melt partitioning, the effects of melt composition cannot be ignored; Goldschmidt's Rules consider only the crystal phase.

B. Use of Ionic Radii to Predict Coordination Number of Cations in Silicate Minerals

Cation coordination number (CN) for silicate minerals is the number of oxygen anions surrounding a cation. If we assume that 1) cations and anions are rigid spheres, and 2) ionic radii are constant, the concept of radius ratio, i.e. (cation ionic radii)/(oxygen ionic radii) can be used to predict cation coordination number (see Figure 5). Figure 6 shows the predicted CN for the alkali metals and alkaline earths. Na, K, Mg and Ca are major elements in rock-forming minerals, such as feldspars and pyroxenes, and their observed CN are accurately predicted by their radius ratio. We will see that the predicted CN for the alkali metals and alkaline earths commonly occurring as TE (i.e., Li, Rb, Cs and Be, Sr, and Ba, respectively) are useful for predicting and understanding the partitioning of these elements between co-existing phases.

Radius Ratio	Arrangement of Anions Around Cations	Cation Coordination Number (CN)
0.15 to 0.22	Corners of equilateral triangle	3
0.22 to 0.41	Corners of tetrahedron	4
0.41 to 0.73	Corners of cube	8
>1	Midpoints of cube edges	12 (close-packing)

Figure 5. Relationship between radius ratio, i.e. (cation ionic radius)/(anion ionic ratios) and cation coordination number for ions that are rigid spheres of uniform size.

Ion	Ionic Radius [a] $(A^o, 10^{-8}$ cm)	Radius Ratio (r_c/r_o^{-2})	Predicted Coordination Number (CN)	Commonly observed CN in minerals
O^{-2}	1.32			
Cs^{+1}	1.96	1.48	12	
Rb^{+1}	1.81	1.37	12	
K^{+1}	1.68	1.27	12	8-12
Ba^{+2}	1.68	1.27	12	
Sr^{+2}	1.48	1.12	12	
Na^{+1}	1.24	0.94	8	6-8
Ca^{+2}	1.20	0.91	8	6-8
Li^{+1}	0.82	0.62	6	
Mg^{+2}	0.80	0.61	6	6
Be^{+2}	0.35	0.26	4	

(a) ionic radius from Whittaker and Muntus (1970)

Figure 6. Predicted coordination numbers based on radius ratio with O^{-2} as the anion for alkali metals and alkaline earths. Note for the major elements K, Na, Mg and Ca the predicted CN agree with observed CN.

C. Source of Ionic Radii (IR)

Since ionic radius is a very useful characteristic for understanding partitioning of trace elements, it is imperative that we know how these values are determined. There are many tabulations of ionic radii; a useful compilation was presented by Shannon and Prewitt, "Effective ionic radii in oxides and fluorides", Acta Crystallographica, B25, 925-946, 1969, and revised by Shannon in Acta Crystallographica A32, 751-767, 1976.

They used interatomic data for simple oxides and fluorides to derive an empirical set of ionic radii which best satisfy the measured interatomic distances. Essentially in a compound AO, one must divide the interatomic distance into the contribution from A^{+2} and O^{-2}.

To do this there are problems to address and assumptions that are made. Specifically:

(1) One important aspect is that in a given mineral the interatomic distance between a given cation and oxygen is not a constant. This is true even for a given site in a mineral. An example of the problem relevant to rock-forming minerals is that in olivine $(Mg, Fe)_2SiO_4$ there are two distinct geometrical positions of (Mg,Fe), known as the M_1 and M_2 sites. The observed metal (Mg/Fe)-oxygen distance ranges from 2.10 to 2.18 A^o for cations in the M_1 site and 2.06 to 2.27A^o for cations in the M_2 site (Birle et al., 1968); the important result is that the metal-oxygen distance is variable. Shannon and Prewitt (1969) used the average interatomic distance measured for oxides and fluorides.

(2) Another issue is that ionic radius of cations are all relative to that of O^{-2}. Traditionally experimental results have indicated 1.40A° for oxygen but calculations suggest 1.26A° for oxygen. Obviously, much larger cation ionic radii result from the latter choice.

(3) Also as expected from coulombic attraction forces, ionic radii estimates vary with increasing coordination number (CN), such that ionic radius increases with coordination number. The effect is about 5-10% as CN increases from 4 to 6 to 8 (e.g. see variation with CN for alkali metals in Figure 7).

Li	Be						
1 IV 0·68 VI 0·82	2 III 0·25 IV 0·35						
Na 1 IV 1·07 V 1·08 VI 1·10 VII 1·21 VIII 1·24 IX 1·40	**Mg** 2 IV 0·66 V 0·75 VI 0·80 VIII 0·97						
K 1 VI 1·46 VII 1·54 VIII 1·59 IX 1·63 X 1·67 XII 1·68	**Ca** 2 VI 1·08 VII 1·15 VIII 1·20 IX 1·26 X 1·36 XII 1·43	**Sc** 3 VI 0·83 VIII 0·95	**Ti** 2 VI 0·94 3 VI 0·75 4 V 0·61 VI 0·69	**V** 2 VI 0·87 3 VI 0·72 4 VI 0·67 5 IV 0·44 V 0·54 VI 0·62	**Cr** 2 VI L 0·81 H 0·90 3 VI 0·70 4 IV 0·52 VI 0·63 5 IV 0·43 6 IV 0·38	**Mn** 2 VI L 0·75 H 0·91 VIII 1·01 3 V 0·66 VI L 0·66 H 0·73 4 VI 0·62 6 IV 0·35 7 IV 0·34	**Fe** 2 IV H 0·71 VI L 0·69 H 0·86 3 IV H 0·57 VI L 0·63 H 0·73
Rb 1 VI 1·57 VII 1·64 VIII 1·68 X 1·74 XII 1·81	**Sr** 2 VI 1·21 VII 1·29 VIII 1·33 X 1·40 XII 1·48	**Y** 3 VI 0·98 VIII 1·10 IX 1·18	**Zr** 4 VI 0·80 VII 0·86 VIII 0·92	**Nb** 2 VI 0·79 3 VI 0·78 4 VI 0·77 5 IV 0·40 VI 0·72 VII 0·74	**Mo** 3 VI 0·75 4 VI 0·73 5 VI 0·71 6 IV 0·50 V 0·58 VI 0·68 VII 0·79	**Tc** 4 VI 0·72	**Ru** 3 VI 0·78 4 VI 0·70
Cs 1 VI 1·78 VIII 1·82 IX 1·86 X 1·89 XII 1·96	**Ba** 2 VI 1·44 VII 1·47 VIII 1·50 IX 1·55 X 1·60 XII 1·68	**La–Lu**	**Hf** 4 VI 0·79 VIII 0·91	**Ta** 3 VI 0·75 4 VI 0·74 5 VI 0·72 VIII 0·77	**W** 4 VI 0·73 6 IV 0·50 VI 0·68	**Re** 4 VI 0·71 5 VI 0·60 6 VI 0·60 7 IV 0·48 VI 0·65	**Os** 4 VI 0·71
Fr	**Ra** 2 VIII 1·56 XII 1·72	**Ac–Lw**					

La	Ce	Pr	Nd	Pm	Sm	Eu
3 VI 1·13 VII 1·18 VIII 1·26 IX 1·28 X 1·36 XII 1·40	3 VI 1·09 VIII 1·22 IX 1·23 XII 1·37 4 VI 0·88 VIII 1·05	3 VI 1·08 VIII 1·22 4 VI 0·86 VIII 1·07	3 VI 1·06 VIII 1·20 IX 1·17	3 VI 1·04	3 VI 1·04 VIII 1·17	2 VI 1·25 VIII 1·33 3 VI 1·03 VII 1·11 VIII 1·15
Ac	**Th** 4 VI 1·08 VIII 1·12 IX 1·17	**Pa** 4 VIII 1·09 5 VIII 0·99 IX 1·03	**U** 3 VI 1·12 4 VII 1·06 VIII 1·08 IX 1·13 5 VI 0·84 VII 1·04 6 II 0·53 IV 0·56 VI 0·81 VII 0·96	**Np** 2 VI 1·18 3 VI 1·10 4 VIII 1·06	**Pu** 3 VI 1·09 4 VI 0·88 VIII 1·04	**Am** 3 VI 1·08 4 VIII 1·03

7ci fhYgm'cZ 9`gYj ]Yfž ëbWž`\hnd.##k k k "gW]YbWX]fYWh'Wca "'I gYX'k]h\'dYfa]gg]cb"

B
3 III 0·10
IV 0·20

C
—

N
—

O
2 II 1·27
III 1·28
IV 1·30
VI 1·32
VIII 1·34

F
1 II 1·21
III 1·22
IV 1·23
VI 1·25

Al
3 IV 0·47
V 0·56
VI 0·61

Si
4 IV 0·34
VI 0·48

P
5 IV 0·25

S
2 IV (1·56)
VI (1·72)
VIII (1·78)
6 IV 0·20

Cl
1 IV (1·67)
VI (1·72)
VIII (1·65)
5 III 0·20
7 IV 0·28

Co
2 IV H 0·65
VI L 0·73
H 0·83
3 VI L 0·61
H 0·69

Ni
2 VI 0·77
3 VI L 0·64
H 0·68

Cu
1 II 0·54
2 IVsq 0·70
V 0·73
VI 0·81

Zn
2 IV 0·68
V 0·76
VI 0·83
VIII 0·98

Ga
3 IV 0·55
V 0·63
VI 0·70

Ge
4 IV 0·48
VI 0·62

As
5 IV 0·42
VI 0·58

Se
2 VI (1·88)
VIII (1·90)
6 IV 0·37

Br
1 VI (1·88)
VIII (1·84)
7 IV 0·34

Rh
3 VI 0·75
4 VI 0·71

Pd
1 II 0·67
2 IVsq 0·72
VI 0·94
3 VI 0·84
4 VI 0·70

Ag
1 II 0·75
IVsq 1·10
V 1·20
VI 1·23
VII 1·32
VIII 1·38
3 IVsq 0·73

Cd
2 IV 0·88
V 0·95
VI 1·03
VII 1·08
VIII 1·15
XII 1·39

In
3 VI 0·88
VIII 1·00

Sn
2 VIII 1·30
4 VI 0·77

Sb
3 IVpy 0·85
V 0·88
5 VI 0·69

Te
4 III 0·60

I
1 VI (2·13)
VIII (1·97)
5 VI 1·03

Ir
3 VI 0·81
4 VI 0·71

Pt
2 IVsq 0·68
4 VI 0·71

Au
3 IVsq 0·78

Hg
1 III 1·05
2 II 0·77
IV 1·04
VI 1·10
VIII 1·22

Tl
1 VI 1·58
VIII 1·68
XII 1·84
3 VI 0·97
VIII 1·08

Pb
2 IVpy 1·02
VI 1·26
VIII 1·37
IX 1·41
XI 1·47
XII 1·57
4 VI 0·86
VIII 1·02

Bi
3 V 1·07
VI 1·10
VIII 1·19

Po
4 VIII 1·16

At

Gd
3 VI 1·02
VII 1·12
VIII 1·14

Tb
3 VI 1·00
VII 1·10
VIII 1·12
4 VI 0·84
VIII 0·96

Dy
3 VI 0·99
VIII 1·11

Ho
3 VI 0·98
VIII 1·10

Er
3 VI 0·97
VIII 1·08

Tm
3 VI 0·96
VIII 1·07

Yb
3 VI 0·95
VIII 1·06

Lu
3 VI 0·94
VIII 1·05

Cm
3 VI 1·06
4 VIII 1·03

Bk
3 VI 1·04
4 VIII 1·01

Cf
3 VI 1·03

Es

Fm

Md

No

Lw

7ci fhYgmcZ 9`gYj]Yfž =bWž \ hnd. ##k k k "gW]Yb W X]fYWh W¢a "´I gYX ك]h\ ´dYfa]gg]cb"

Figure 7. Periodic Table, showing for naturally occurring elements, their ionic radius (10^{-8} cm, angstroms) for various oxidation states (1, 2, 3, etc.) and commonly observed coordination numbers (IV, VI, VIII and XII). For Cr^{+2}, Mn^{+2}, Fe^{+2}, Fe^{+3} and Co^{+2} the symbols H and L indicate high and low spin states (to be discussed). Data are from Whittaker and Muntus (1970).

D. Adaptation of Ionic Radii Inferred From Simple Compounds to Silicate Minerals

Whittaker and Muntus (1970) in a paper titled "Ionic radii for use in geochemistry" used the two sets of ionic radii presented by Shannon and Prewitt (1969) and evaluated their consistency in predicting the coordination numbers observed in silicate minerals. They concluded that the best fit to observed coordination number is an intermediate set of ionic radii based on a radius of $O^{-2} = 1.32A°$. Figure 7 is a periodic table indicating the ionic radii recommended by Whittaker and Muntus (1970) for elements in different oxidation states and coordination numbers. This table, i.e., Figure 7, should be studied carefully. Note the following systematics:

1. For a given element, cation radius decreases with increasing charge and increases with increasing CN (e.g., see variation with CN for alkali metals in Figure 7).

2. In a periodic table group the IR increases with increasing Z because the effect of adding a nuclear charge is overwhelmed by adding an outer electron to a more distant orbital (e.g., alkali metals in CN 6 increase from 0.82 (Li) to 1.78 (Cs) (Figure 4).

4. Across a period in the table, cations of same electronic structure decrease in ionic radius, e.g. Na^{+1}, Mg^{+2}, Al^{+3}

5. In first transition metal series ionic radii do not vary systematically with atomic number (Figure 8); their ionic radii reflect crystal field effects (to be discussed).
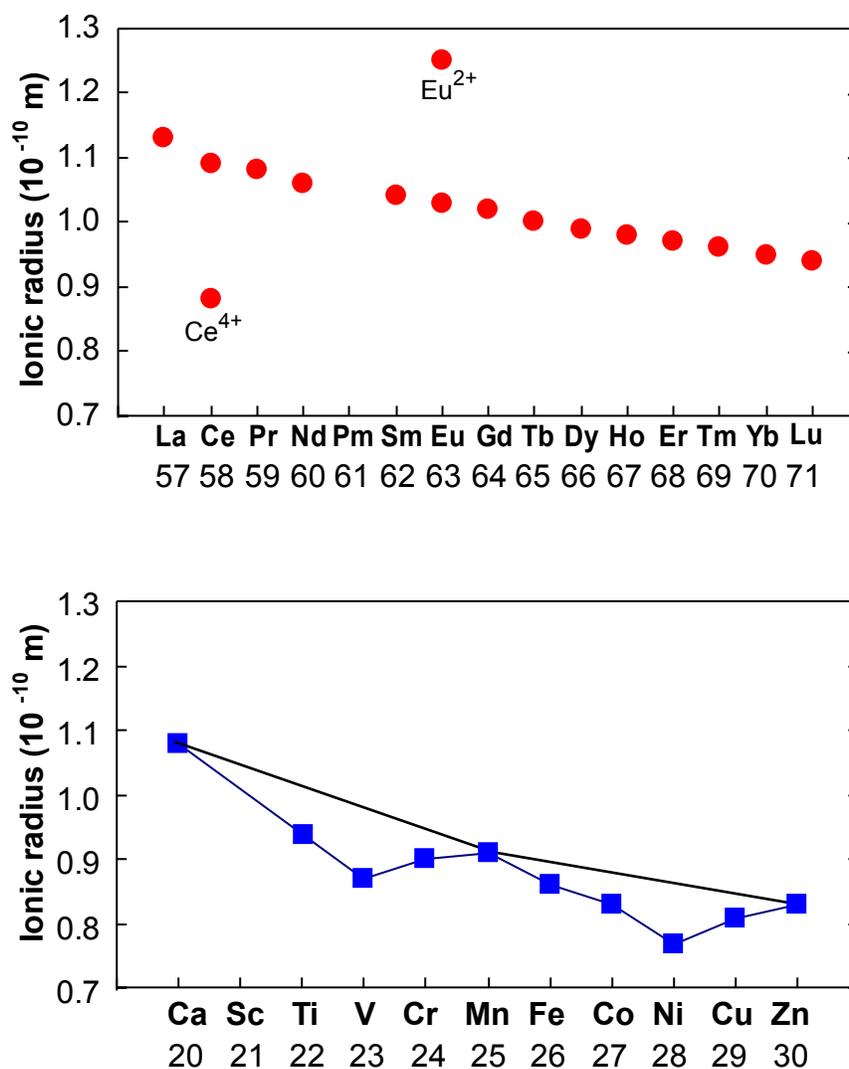
Figure 8. Upper: ionic radii of +3 rare-earth element ions for CN VI as a function of atomic number 57-71. The steady decrease is known as the lanthanide contraction. Also note the anomalous radii of naturally occurring Ce^{+4} and Eu^{+2}.

Lower: Ionic radii of +2 first series transition metals for CN VI. While there is a steady decrease from Ca^{+2} to Mn^{+2} to Zn^{+2}, the overall trend is complex showing a maximum at Mn^{+2}.

6. A particularly systematic decrease in +3 ionic radii occurs across the lanthanide series (Figure 8 - upper). This is because the electron configuration of the lanthanides, i.e., rare-earth elements, includes electrons in 4f orbitals (Figure 1). These 4f electrons are shielded by outer electrons; i.e. they are located closer to nucleus than 5s and 6p electrons. An important consequence of the REE differing only in the number of 4f electrons and their ubiquitous +3 oxidation state is that the chemical and geochemical behavior of individual rare-earth elements (REE) are quite similar. In fact it was difficult for chemists to isolate and identify all of these elements with $Z = 57$ to 71 (e.g., Yb and Lu were not identified until 1907-08). However, the systematic decrease in ionic radii of their +3 ions, known as the lanthanide contraction, enables minerals to discriminate between REE. In particular, the relative abundance of REE change during partial melting because most minerals prefer either the larger or smaller REE ions.

Another important effect of the lanthanide contraction is shown by the following table of of ionic radii for CN VI.

Sc^{+3} 0.83	Ti^{+4} 0.69	V^{+5} 0.62
Y^{+3} 0.98	Zr^{+4} 0.80	Nb^{+5} 0.72
La^{+3} 1.15	Hf^{+4} 0.79	Ta^{+5} 0.72

We see the expected decrease in ionic radius as Atomic Number increases from Sc to Y to La, but because of the lanthanide contraction Zr and Hf as

well as Nb and Ta have very similar ionic radii; this is a result of "filling" the 4f orbitals to form the REE (Z = 57 to 71) between Zr and Hf (Z = 40 and 72, respectively) and between Nb and Ta (Z = 41 and 73, respectively) (see Figure 1). This result explains why Zr and Hf as well as Nb and Ta behave very similarly in terrestrial and lunar rocks. Until recently it was believed that Zr/Hf and Nb/Ta abundance ratios are quite constant in most natural materials. With the precise abundance data for these elements now determined by mass spectrometry, we now know that there are significant variations in Zr/Hf and Nb/Ta which reflect specific processes (e.g., see Pfänder et al., 2007).

E. First Series Transition Metals: Crystal Field Theory

(Reference: Mineralogical Applications of Crystal Field Theory by R.G. Burns, Cambridge UiversityPress (1993)

1. Crystal field theory is an ionic model which treats cations and anions as point charges and considers the interaction of the negative anion charges with the electron orbitals of the cation.

2. It is particularly useful for understanding transition metal geochemistry, in particular the ionic radius and partition coefficient variations as a function of atomic number.

3. The first series transition metals Sc through Zn are characterized by an electron configuration involving an [Ar] core plus 3d and 4s electrons (Figure 1); i.e., the electron configuration of the atoms are:

$^{21}Sc(3d^14s^2)$ $Ti(3d^24s^2)$ $V(3d^34s^2)$ $Cr(3d^54s^1)$

$Mn(3d^54s^2)$ $Fe(3d^64s^2)$ $Co(3d^74s^2)$ $Ni(3d^84s^2)$

$Cu(3d^{10}4s1)$ $Zn(3d^{10}4s^2)$
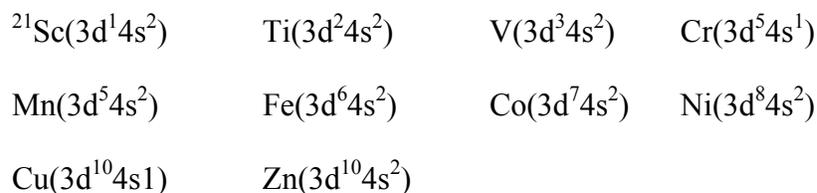
4. Now if we make various ions by removing electrons, the ions have different numbers of "d" electrons, e.g.:

$Sc^{+3}(3d^0)$ $Ti^{+4}(3d^0)$ $V^{+5}(3d^0)$ $V^{+3}(3d^2)$ $Cr^{+3}(3d^3)$ $Cr^{+2}(3d^4)$ $Mn^{+2}(3d^5)$

$Fe^{+3}(3d^5)$ $Fe^{+2}(3d^6)$ $Co^{+2}(3d^7)$ $Ni^{+2}(3d^8)$ $Cu^{+2}(3d^9)$ $Zn^{+2}(3d^{10})$
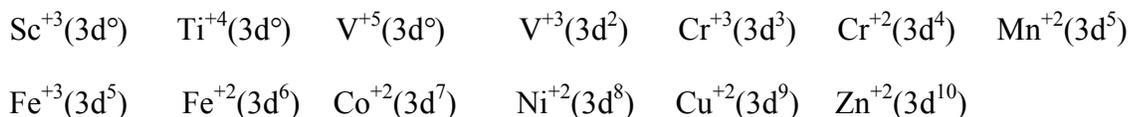
5. Energy levels of d orbitals: There are 10 d electrons, 2 each to an orbital. These 5 orbitals are uniform in energy (E) if not surrounded by anions, i.e.,
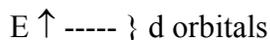
$$E \uparrow ----- \} \text{ d orbitals}$$

However, if these orbitals are in an environment surrounded by anions with a specific geometry the energy levels of the orbitals change; e.g. consider an octahedral environment and the interaction between the octahedrally coordinated anions with the distinctive spatial electron density distributions of the five 3d orbitals (Figure 9). In this case the orbitals d_{z^2} and $d_{x^2-y^2}$ are oriented directly toward anions whereas the orbitals d_{xy}, d_{yz} and d_{xz} are directed between anions (Figure 9). As a result the ionic radii of the first series transition elements do not systematically decrease with increasing atomic number; that is when the d_{z^2} and $d_{x^2-y^2}$ orbitals are occupied (e.g., Cr^{+2} and Cu^{+2}), their inferred ionic radii are anomalously large (Figure 8, lower).

Sketch showing six negative charges arranged octahedrally
around a central M^{+2} ion with a set of Cartesian axes for reference.

Representation of the "shape" of electron clouds for various
types of atomic orbitals.
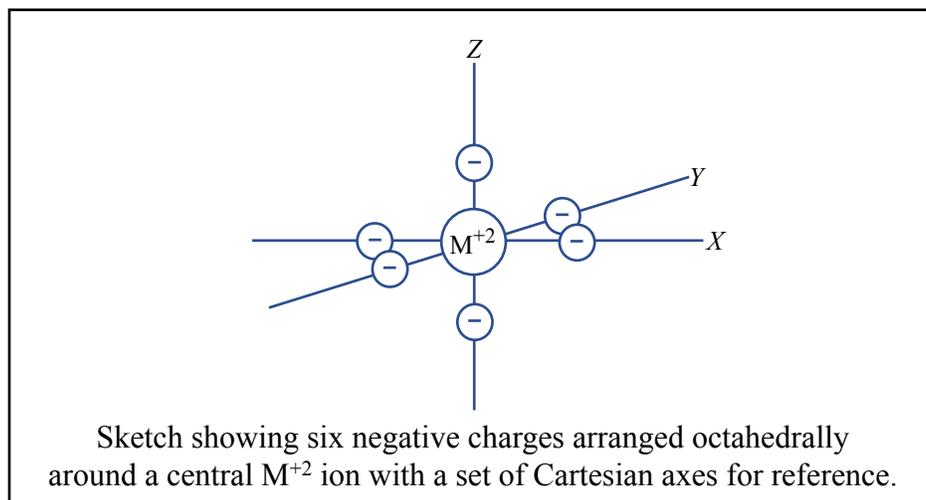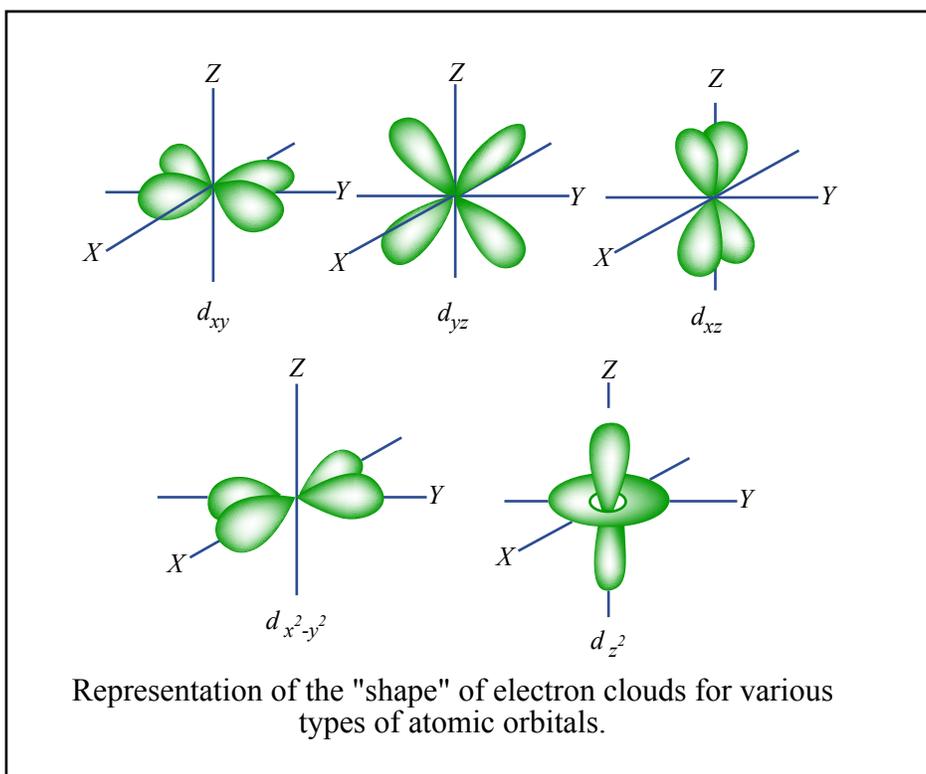
Figure 9.   Upper: Octahedrally coordinated anions (negative changes) surrounding a metal cation (M^{+2}).

Lower: Spatial distribution of the five d orbitals. Note that in an octahedral environment (upper), the orbitals $d_z{}^2$ and $d_x{}^2{}_{-y}{}^2$ are oriented directly toward anions whereas the peaks in electron density of the orbitals d_{xy}, d_{yz} and d_{yz} are directed between the anions.

Another result of the spatial orientation of d orbitals and their interactions with anions is that the relative energy levels of the five d orbitals change; that is, in an octahedral environment the d_z2 and $d_x2_{-y}2$ orbitals have higher energies than the d_{xy}, d_{xz} and d_{yz} orbitals. This energy difference is the Crystal Field Splitting Energy (Δ_o) with the d_z2 and $d_x2_{-y}2$ orbitals offset to a higher energy level ($0.6\ \Delta_o$), because they are directed toward the anions, whereas the d_{xy}, d_{yz} and d_{yz}, because they are oriented between the octahedrally coordinated anions, are offset ($0.4\ \Delta_o$) to a lower energy level.   That is:
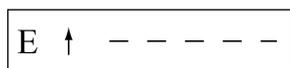
E ↑ − − − − −   becomes in an octahedral environment
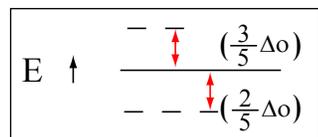
E ↑   − ↨ $(\frac{3}{5}\Delta o)$ where Δ_o is the energy difference between the two sets of

− − ↨ $(\frac{2}{5}\Delta o)$

orbitals.

Now consider the energy levels for d orbitals for Mn^{+2} and Fe^{+3}, two ions with five d electrons:

There are two possible scenarios.

E ↑   ↨ ↨   − −
     ↑ ↑ ↑   or   ↑↓ ↑↓ ↑
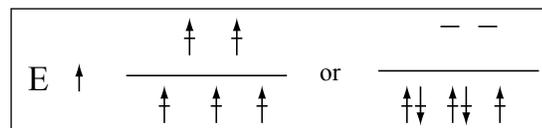
The left diagram is the high electron spin case, one electron per orbital, and the net crystal field stabilization energy is zero. The right diagram is the low electron spin case, paired electrons in two orbitals, and the crystal field stabilization energy is 2 Δ_o (five times $0.4\Delta_o$). Whether electrons are paired, low spin case, or populate the higher energy levels, high spin case, depends upon the energy required to pair electrons in an orbital; that is, is the P (pairing energy) less than or greater than Δ_o, the crystal field splitting energy)?

For most silicate minerals $\Delta_o < P$ at low pressures, so we have the high spin state, but as pressure increases Δ_o may exceed P and the low spin state is preferred.

Similarly, there are Low and High spin configurations of Fe^{+2} which has six d electrons
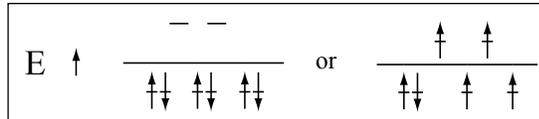
Because Fe is abundant in the earth's mantle, the existence of high or low spin states is significant because in these different spin states Fe has different physical-chemical properties. At low pressure Δ_o is <P so the high spin state is favored, but with increasing pressure the Crystal Field Splitting Energy (Δ_o) increases; eventually with increasing pressure the low spin state is favored. The possible important consequences are discussed by Lin et al., 2007.

12.479 Trace-Element Geochemistry

Spring 2013